ARMY RESEARCH LABORATORY

Computational Characterization of 2-Azidocycloalkanamines: Notional Variations on the Hypergol 2-Azido-N,N-Dimethylethanamine (DMAZ)

by Michael J. McQuaid

ARL-TR-2806

September 2002

NOTICES

Disclaimers

The findings in this report are not to be construed as an official Department of the Army position unless so designated by other authorized documents.

Citation of manufacturer's or trade names does not constitute an official endorsement or approval of the use thereof.

Destroy this report when it is no longer needed. Do not return it to the originator.

Army Research Laboratory
Aberdeen Proving Ground, MD 21005-5066

ARL-TR-2806 **September 2002**

Computational Characterization of 2-Azidocycloalkanamines: Notional Variations on the Hypergol 2-Azido-N,N-Dimethylethanamine (DMAZ)

Michael J. McQuaid
Weapons and Materials Research Directorate, ARL

Abstract

The fuel 2-azido-N,N-dimethylethanamine (DMAZ) has shown considerable promise as a replacement for hydrazine-based fuels in hypergolic propulsion systems, but the ignition delays observed for DMAZ-inhibited red fuming nitric acid (IRFNA) systems are longer than those for monomethylhydrazine-IRFNA systems. This report considers the potential of 2-azidodocycloalkanamine-based fuels for addressing this issue. Such molecules have two stereochemically distinct isomers, one of which prevents the azide group from "shielding" the amine lone pair electrons from proton attack. The other promotes such shielding. Since shielding likely influences the manner in which nitric acid reacts with amine-azide fuels, the ignition delays for the isomers may be different, and it is possible that one of the isomers will yield shorter ignition delays than DMAZ. To support consideration of the synthesis and development of 2-azido-N,N-dimethylcyclopropanamine (ADMCPA) equilibrium structures are identified and their gas-phase heats of formations estimated via density functional theory-based calculations. In addition, ADMCPA isomer condensed-phase densities and heats of vaporization are estimated via molecular dynamics simulations performed with halogen analogs. Combined and employed to predict ballistic properties, the computational results indicate that the ADMCPA isomers merit further investigation as hypergols. A suggestion for synthesizing *cis*-ADMCPA is also proffered.

Acknowledgments

Mr. D. Thompson (U.S. Army Aviation and Missile Command [AMCOM]) proposed proton attack of 2-azido-N,N-dimethylethanamine's (DMAZ's) amine lone pair electrons as an important step in the ignition of a DMAZ-inhibited red fuming nitric acid (IRFNA) system, raising steric shielding as an issue to be examined. The general idea of introducing a cyclic or bridging structure into DMAZ to prevent shielding was suggested by Dr. C. Chabalowski (U.S. Army Research Laboratory [ARL]) during one of our many discussions over the theoretical results obtained for DMAZ. Dr. N. Reynolds (Accelrys, Inc.) wrote the "script" employed to run the molecular dynamics simulations. Dr. S. Bunte (ARL) offered many helpful suggestions with respect to running the Accelrys polymer software codes. Dr. A. Kotlar (ARL) performed the I_{SP} calculations presented. The vast majority of the calculations reported were performed at the Department of Defense Major Shared Resource Center at Aberdeen Proving Ground.

INTENTIONALLY LEFT BLANK.

Contents

INTENTIONALLY LEFT BLANK.

List of Figures

INTENTIONALLY LEFT BLANK.

List of Tables

INTENTIONALLY LEFT BLANK.

1. Introduction

Providing an extremely reliable basis on which to design intermittent and/or variable thrust propulsion systems, hypergolic liquid (or gel) fuel-oxidizer combinations—i.e., those that react spontaneously upon mixing—are employed throughout the Department of Defense (DOD) and National Aeronautics and Space Administration (NASA) for aviation and missile applications. One of the drawbacks to many "standard" hypergolic fuel-oxidizer combinations, however, is that the fuels are derived from hydrazine, monomethylhydrazine (MMH), and/or unsymmetrical dimethylhydrazine (UDMH)—all of which are acutely toxic and suspected carcinogens [1]. Searching for alternatives to hydrazine-based fuels, the Army (via the U.S. Army Aviation and Missile Command [AMCOM] and in collaboration with other DOD and NASA organizations) is investigating the use of various 2-azidoethanamines in such applications. Collectively referred to as Competitive Impulse Non-Carcinogenic Hypergols (CINCH) [2], the formulation within this class of compounds receiving the most attention is 2-azido-N,N-dimethylethanamine ($(CH_3)_2NCH_2CH_2N_3$). Also referred to as DMAZ, this fuel has been found to yield performance competitive with Aerozine 50 (a 50/50 mixture of hydrazine and UDMH) in inhibited red fuming nitric acid (IRFNA) oxidized experimental systems. DMAZ-IRFNA systems do not, however, meet "ignition delay" standards set by MMH-IRFNA systems, and this shortcoming may negatively impact the Army's ability to field this alternative.

Based on traditional chemical knowledge and testing performed for AMCOM, it was concluded that a rate-limiting step in DMAZ-IRFNA ignition might be associated with an initial chemical reaction—namely, proton transfer from nitric acid to DMAZ's amine nitrogen [3]. As a result, one of the approaches to addressing the ignition delay issue has been to synthesize differently substituted 2-azidoethanamines with the hope of enhancing the amine's reactivity/basicity. Two compounds synthesized subsequent to the identification of DMAZ as a promising hypergol are 2-azido-N-methylethanamine (MMAZ) and 2-azido-N-cyclopropylethanamine (CPAZ), and a comparison of their attributes is instructive. MMAZ, which has a hydrogen atom in lieu of one of the methyl groups in DMAZ, is not hypergolic, while CPAZ, which has a cyclopropyl group in lieu of the methyl group in MMAZ, is. However, the hypothesis that the ignition delays for these fuels are, in fact, due to differences in the basicity of their amine nitrogen remains to be proven.

In support of the experimentally based research being pursued through AMCOM, the U.S. Army Research Laboratory (ARL) is employing computational quantum chemistry in an attempt to identify the differences between fuels that correlate with ignition delay, the initial focus of this effort being the characterization of fuel-nitric acid proton transfer reactions. Toward characterizing DMAZ-nitric acid reactions, a study to establish the nature of DMAZ equilibrium structures was conducted [4], with 12 conformers being identified via density functional theory

(DFT). One of the interesting findings of that study was that in DMAZ's lowest energy structure (Figure 1), the azido group will shield the amine lone pair electrons from proton attack. Given the importance of proton transfer reactions inferred from experiments, this finding raised the possibility of molecular geometry having an influence in the ignition process.

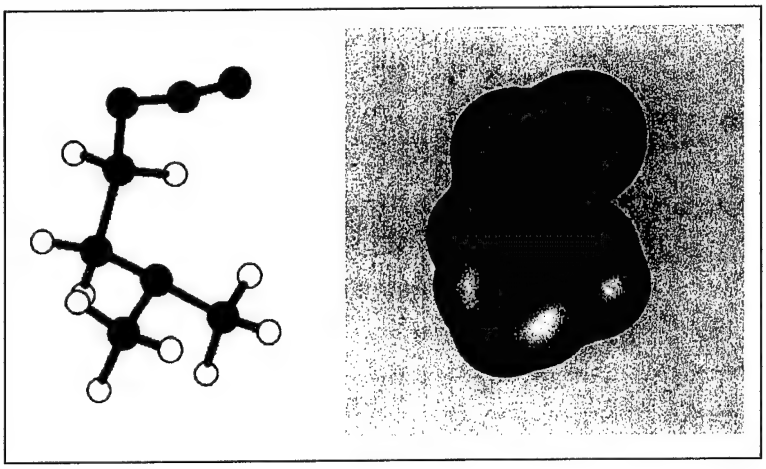

Figure 1. The lowest energy DMAZ structure and a mapping of the electrostatic potential on its 0.004 atomic unit (a.u.) electron isodensity surface. Dark blue regions of the potential correspond to nucleophilic (lone pair electron) sites.

While considering means to explore this possibility, doubts about the value of a computational study arose, the concern being that even if a deleterious relationship between shielding and ignition delay could be established, an inability to prevent shielding would make the knowledge moot. This prompted the author to consider alternatives to 2-azidoethanamines. Informed that the introduction of a cyclic structure can "lock in" a preferred orientation between functional groups, the author sketched out a number of notional molecules based on the approach. Of the molecules sketched, 2-azidocycloalkanamines, the *trans* form of which prevents the azide group from coming in close proximity to the amine lone pair, were intuitively appealing. Stoichiometrically, 2-azido-N,N-dimethylcyclopropanamine (ADMCPA), 2-azido-N-methylcyclobutanamine (AMCBA), and 2-azidocyclopentanamine (ACPA) differ from DMAZ by only one carbon atom, ($C_5H_{10}N_4$ vs. $C_4H_{10}N_4$), and, like DMAZ, the amine and azide groups are separated by two carbon atoms. Moreover, like CPAZ, which also has $C_5H_{10}N_4$ stoichiometry, the cycloalkyl group should increase the reactivity of the amine lone pair. Therefore, if shielding of these electrons by the azido group is indeed a rate-determining mechanism in the ignition process, the *cis* and *trans* forms of a given azidocycloalkanamine will have different ignition delays, and it is possible that one of the forms will yield shorter ignition delays than DMAZ or CPAZ. AMCBA and ACPA will presumably be less reactive than ADMCPA, but might be worth synthesizing if ADMCPA proves to react too violently—a problem encountered in CINCH molecules synthesized with more than one azide functional group [2, 3].

It is, of course, a nontrivial exercise to experimentally synthesize and characterize a new compound, and the intuition of a computational chemist is hardly adequate justification for undertaking such a project. Therefore, computationally based property predictions were obtained to support consideration of 2-azidocycloalkanamine synthesis. Included are DFT-based characterizations of *trans* and *cis* ADMCPA equilibrium structures and their gas-phase heat of formation. A limited set of equilibrium AMCBA and ACPA conformers is also characterized. In addition, an approach to estimating the condensed-phase densities and heats of vaporization for azide-functionalized compounds based on molecular dynamics (MD) simulations with halogen analogs is proposed and validated, then employed to predict condensed-phase properties for the ADMCPA isomers. The property predictions are subsequently employed in ballistic performance calculations that provide a comparison of ADMCPA isomer specific impulses (I_{SP}) and density specific impulses (D^*I_{SP}) relative to those for the CINCH fuels and MMH. Finally, a suggestion for synthesizing *cis*-ADMCPA is proffered.

2. Computational Quantum Chemistry Methods

The Gaussian98 (G98) suite of quantum chemistry codes [5] was employed to identify equilibrium ADMCPA, AMCBA, and ACPA structures and characterize their normal modes. The level of theory employed—DFT utilizing the B3LYP exchange-correlation functionals [6–8] and 6-311++G(d,p) atomic orbital basis set [9–11] on a G98-defined "ultrafine" grid—was chosen based on the success achieved with it in characterizing DMAZ [4]. In addition to the structural characterizations, estimates of gas-phase heats of formation at 298 K ($\Delta H_f(298)$) were sought for use in predicting ballistic performance. Unfortunately, the well-established approach for obtaining $\Delta H_f(298)$ estimates via the G2 method [12] proved computationally intractable, necessitating the implementation of an alternate method. The results presented in this report are derived from the heats of reaction ($\Delta H_r(0)$) calculated for "isodesmic" reactions at 0 K. (Isodesmic reactions are those in which the total number of each type of bond are equal in reactants and products; the success of the method assumed to be associated with the cancellation of errors achieved through equating product and reactant bonds [13].) In an attempt to identify if the method generated systematic errors, a variety of reactions involving the formation of molecules of interest and xH_2 ($x = 1$ or 2) from reactants with accepted $\Delta H_f(298)$ values were constructed and their $\Delta H_f(298)$ predictions compared. The zero-point corrected energies and enthalpy differences at 298 and 0 K ($H(298)-H(0)$) for the reactants and reference elements needed to derive $\Delta H_f(298)$ from $\Delta H_r(0)$ were completed at the same level of theory as that employed to characterize the aliphatic amine azides of interest. The author also notes that though "accepted" $H(298)-H(0)$ values are reported in the Joint Army-Navy-NASA-Air Force (JANNAF) thermochemical tables [14] for the reference elements (N_2, H_2, and C(=solid)) and a small subset of the reactants (NH_3 and CH_4), for internal consistency, the $H(298)-H(0)$ values

determined via the quantum chemical calculations are employed in all cases except C(solid). (*H(298)-H(0)* values for C(solid) are not calculable via the theoretical methods employed.)

3. Computational Quantum Chemistry Results

3.1 ADMCPA

Figures 2 and 3 show, respectively, the equilibrium *trans*-ADMCPA and *cis*-ADMCPA structures identified through this study. The geometric parameters for these conformers are provided in Table 1, and Table 2 presents their zero-point corrected energies, dipole moments, and rotational constants. Beyond their classification as *trans* and *cis* forms, the conformers are distinguished by the (dihedral angle) orientations of the $(CH_3)_2N$- and $-N_3$ groups about $(CH_3)_2N$-(C_3H_4) and (C_3H_4)-N_3 bonds, and the labeling scheme was chosen such that alphabetically adjacent conformers are nominally transformed into one another by a dihedral angle rotation about one of these bonds. The scheme also groups conformers based on their H10-C9-N11-C12 angle's proximity to one of three values. For *trans*-ADMCPA, these angles are −67° (*t*-A and *t*-B), 61° (*t*-C and *t*-D), and −165° (*t*-E and *t*-F). Conformers *t*-A and *t*-B are observed to be more than 4 kcal/mol lower in energy than the other conformers, indicating that the −67° H10-C9-N11-C12 angle is energetically favored. (In this configuration, the amine lone pair points toward and directly over the -(C_3H_4)- group.) Two different N2-N3-C4-C6 dihedral angles are also observed, 87° (*t*-A, *t*-D, and *t*-E) and −165° (*t*-B, *t*-C, and *t*-F), but for conformer pairs where this is the only primary difference—(*t*-A, *t*-B), (*t*-C, *t*-D), and (*t*-E, *t*-F)—the energy differences are small (≤0.2 kcal/mol). The six *trans* conformers identified are all of the structures that can be constructed from combinations of the geometric preferences observed. Based on a Boltzmann distribution calculated from *trans* conformer zero-point corrected energies, it is expected that *t*-A (58%) and *t*-B (41%) populations will dominate a gas-phase *trans*-ADMCPA sample at room temperature.

The *cis*-ADMCPA conformers have energetically favored H10-C9-N11-C12 and N2-N3-C4-C6 angles similar to those seen in the *trans*-ADMCPA conformers, but the correspondences between conformer energies and these angles are slightly different. Perhaps the most noteworthy difference is the 1.0 kcal/mol difference between conformers *c*-A and *c*-B. This difference is presumably related to the fact that *c*-A has a (stabilizing) azide-amine interaction similar to that observed in the lowest energy DMAZ conformer (Figure 1). In DMAZ, the conformer with this configuration is also lower in energy than otherwise similar conformers by 1.0–1.3 kcal/mol. Therefore, it is expected that *c*-A will prove to be the lowest energy *cis*-ADMCPA conformer. The six *cis* conformers identified are all of the structures that can be constructed from combinations of the geometric preferences observed. Based on a Boltzmann distribution calculated from *cis* conformer zero-point corrected energies, it is expected that *c*-A (82%) and *c*-B (18%) populations will dominate a gas-phase *cis*-ADMCPA sample at room temperature.

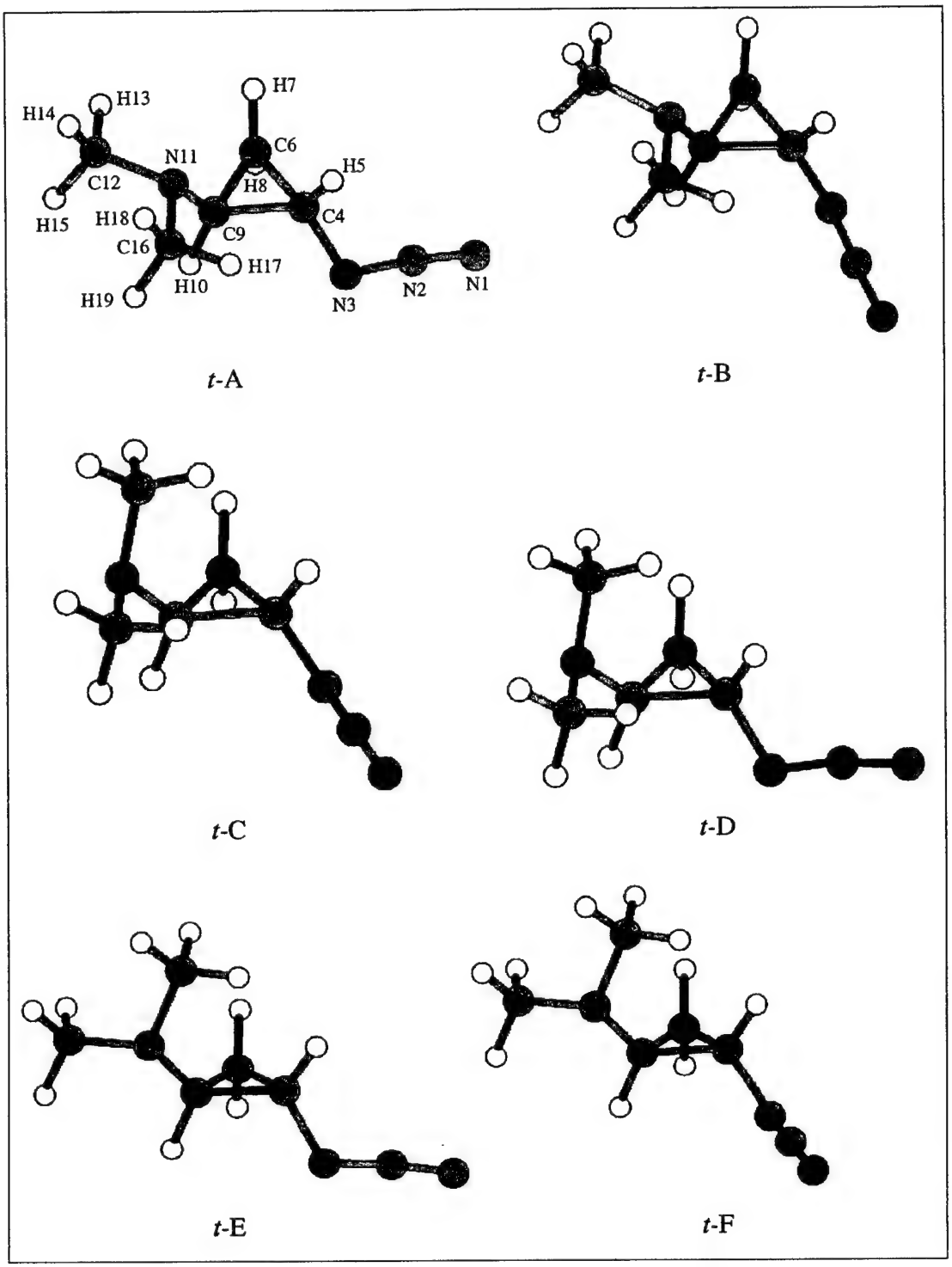

Figure 2. Equilibrium *trans*-ADMCPA conformers.

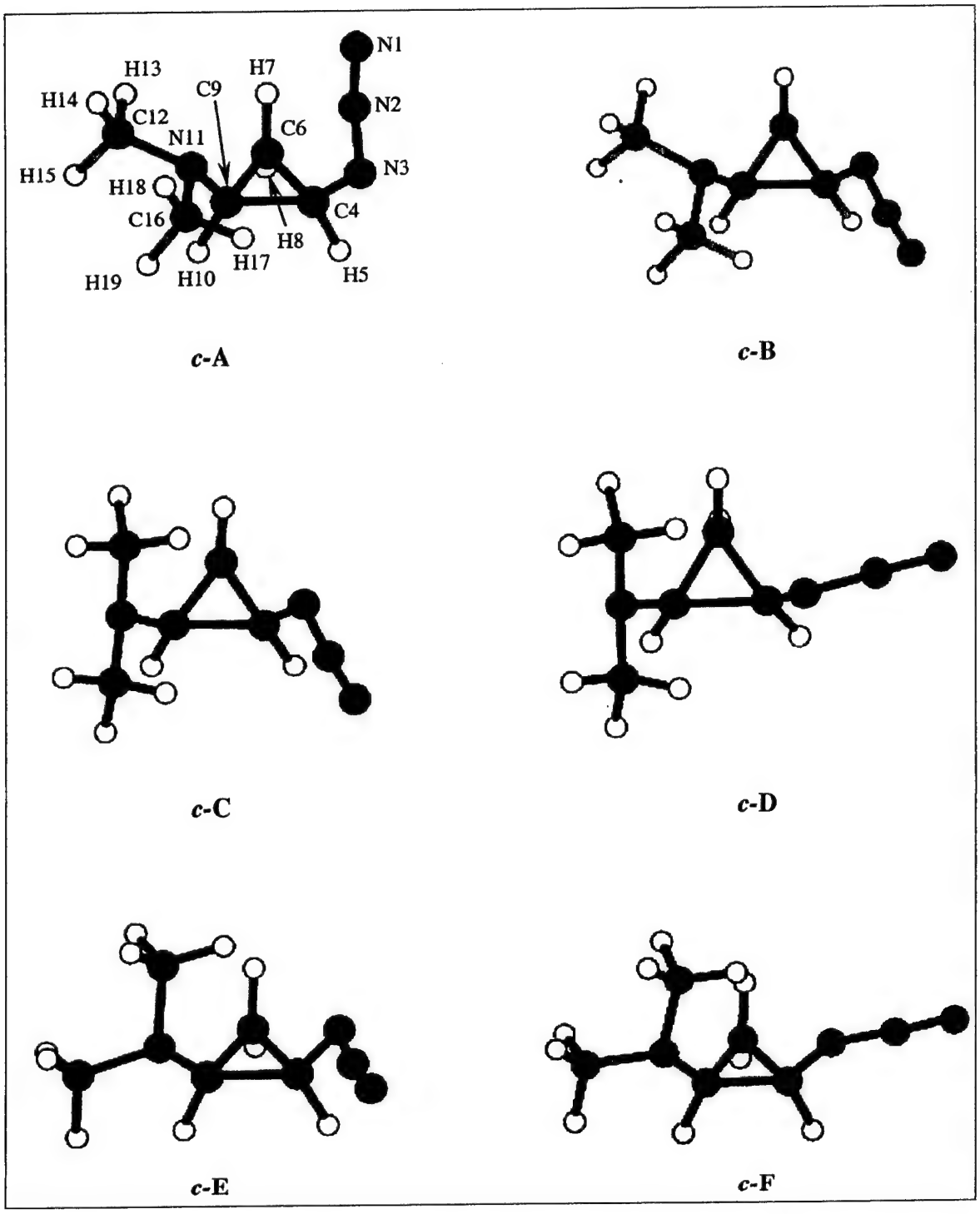

Figure 3. Equilibrium *cis*-ADMCPA conformers. (H8 of conformers *c*-B and *c*-C is hidden in the perspectives shown.)

Table 1. Geometric parameters for equilibrium ADMCPA conformers as computed via B3LYP/6-311++G(d, p).

	trans conformers						*cis* conformers					
Parameter[a]	*t*-A	*t*-B	*t*-C	*t*-D	*t*-E	*t*-F	*c*-A	*c*-B	*c*-C	*c*-D	*c*-E	*c*-F
Bond Length (in Angstroms)												
N1-N2	1.134	1.135	1.136	1.135	1.134	1.134	1.135	1.136	1.136	1.135	1.134	1.135
N2-N3	1.232	1.232	1.231	1.233	1.233	1.233	1.228	1.230	1.230	1.231	1.234	1.231
N3-C4	1.456	1.456	1.456	1.457	1.458	1.458	1.450	1.451	1.453	1.455	1.453	1.455
H5-C4	1.086	1.086	1.086	1.086	1.085	1.085	1.082	1.087	1.087	1.087	1.087	1.087
C6-C4	1.515	1.498	1.504	1.521	1.521	1.504	1.506	1.498	1.503	1.518	1.507	1.524
H7-C6	1.083	1.083	1.082	1.083	1.084	1.083	1.084	1.083	1.083	1.082	1.083	1.083
H8-C6	1.083	1.083	1.083	1.083	1.083	1.083	1.083	1.083	1.083	1.084	1.084	1.084
C9-C6	1.510	1.510	1.503	1.504	1.526	1.528	1.513	1.509	1.502	1.504	1.519	1.500
C9-C4	1.495	1.513	1.531	1.510	1.487	1.504	1.517	1.524	1.544	1.522	1.517	1.500
H10-C9	1.095	1.095	1.086	1.087	1.086	1.085	1.096	1.097	1.088	1.088	1.084	1.085
N11-C9	1.436	1.436	1.439	1.440	1.441	1.442	1.432	1.432	1.432	1.436	1.445	1.442
C12-N11	1.460	1.461	1.459	1.459	1.455	1.456	1.460	1.460	1.458	1.459	1.459	1.460
H13-C12	1.092	1.092	1.093	1.093	1.090	1.091	1.092	1.091	1.093	1.094	1.090	1.088
H14-C12	1.093	1.093	1.093	1.093	1.092	1.092	1.093	1.093	1.093	1.093	1.092	1.093
H15-C12	1.105	1.105	1.105	1.104	1.104	1.105	1.105	1.105	1.103	1.101	1.104	1.105
C16-N11	1.460	1.460	1.455	1.455	1.460	1.460	1.461	1.460	1.456	1.456	1.460	1.461
H17-C16	1.092	1.092	1.090	1.091	1.093	1.093	1.091	1.091	1.091	1.091	1.092	1.093
H18-C16	1.093	1.093	1.092	1.092	1.093	1.093	1.093	1.092	1.093	1.093	1.092	1.092
H19-C16	1.105	1.105	1.105	1.106	1.105	1.104	1.105	1.106	1.101	1.101	1.105	1.105
Simple Angle (in Degrees)												
N1-N2-N3	172.9	172.9	173.2	173.1	173.0	172.9	172.2	172.7	173.1	173.0	172.3	173.1
N2-N3-C4	116.0	116.1	116.3	115.9	115.8	116.0	118.8	116.6	116.4	116.1	115.9	115.7
N3-C4-H5	115.1	115.4	100.6	102.5	102.8	101.9	109.1	114.4	114.6	114.4	114.0	113.3
N3-C4-C6	119.9	116.3	116.6	120.1	120.2	116.7	123.6	116.0	115.4	118.5	116.4	120.1
C4-C6-H7	116.7	117.1	117.0	116.6	116.2	116.5	117.2	114.9	114.8	115.7	115.4	115.4
C4-C6-H8	117.8	116.9	117.1	118.0	118.3	117.5	118.3	119.0	119.1	118.8	118.7	119.0
C4-C6-C9	59.3	60.4	61.2	59.9	58.4	59.5	60.3	60.9	61.8	60.5	60.2	58.9
C4-C9-H10	114.7	115.4	113.1	112.5	112.9	113.4	115.6	113.9	111.8	112.3	112.9	111.8
H10-C9-N11	117.2	117.2	111.5	111.5	111.3	111.2	116.8	116.2	111.3	111.3	111.2	109.8
C9-N11-C12	112.2	112.2	111.6	111.4	116.8	116.8	112.8	112.3	112.9	112.6	116.5	117.0
N11-C12-H13	109.8	109.8	109.7	109.7	99.7	110.6	109.9	109.9	109.6	109.5	110.6	110.5
N11-C12-H14	109.5	109.5	109.6	109.5	146.6	108.6	109.5	109.4	109.5	109.4	108.6	108.5
N11-C12-H15	112.8	112.8	113.1	113.1	102.5	113.9	112.7	112.9	113.8	113.3	112.8	112.8
C9-N11-C16	112.0	112.2	117.3	117.1	110.9	110.9	111.9	112.2	118.9	119.2	111.9	111.1
N11-C16-H17	109.8	109.9	110.5	110.5	109.7	109.7	109.6	110.2	110.1	110.1	110.1	110.1
N11-C16-H18	109.5	109.6	108.6	108.6	109.5	109.5	109.5	109.5	108.3	108.1	109.2	109.1
N11-C16-H19	112.8	112.8	114.0	114.0	27.6	113.0	112.6	112.7	114.1	114.3	113.2	113.1
Dihedral Angle (in Degrees)												
N1-N2-N3-C4	174.8	−172.6	−172.0	173.1	175.9	−173.5	−172.0	171.7	173.9	−169.1	168.7	−172.2
N2-N3-C4-H5	−60.9	50.6	50.9	−57.6	−59.1	55.8	157.0	−49.7	−47.6	51.7	−59.9	51.6
N2-N3-C4-C6	87.5	−165.8	−167.0	89.4	86.6	−163.3	37.0	167.4	169.2	-96.1	157.0	−94.4
N3-C4-C6-H7	−146.8	−141.2	−138.0	−143.8	−144.9	−139.6	−4.7	−5.6	−2.0	2.9	−2.9	−2.3
N3-C4-C6-H8	−2.0	2.7	3.4	−1.5	−1.6	2.9	139.7	137.8	138.9	145.0	138.8	140.3
N3-C4-C6-C9	105.3	110.7	110.4	105.0	105.0	110.2	−110.7	−112.5	−111.8	−106.3	−111.5	−109.7
N3-C4-C9-H10	−4.5	1.0	−0.1	−5.5	−7.1	−2.0	−139.3	−149.0	−150.2	−144.8	−148.4	−143.7
C6-H10-C9-N11	−144.9	−145.6	147.9	−146.1	−145.5	−146.1	−145.3	−146.8	147.8	−146.7	−143.4	−145.2
H10-C9-N11-C12	−66.6	−67.4	60.8	61.7	169.0	169.0	−68.1	−69.5	65.4	68.9	−154.9	−168.7
C9-N11-C12-H13	−55.6	−55.5	−51.1	−51.1	−58.6	−58.8	−55.6	−56.0	−47.1	−48.0	−54.2	−53.9
C9-N11-C12-H14	−174.4	−174.2	−169.6	−169.6	−172.4	−176.3	−174.4	−174.7	−165.3	−166.0	−172.4	−172.2
C9-N11-C12-H15	65.1	65.3	69.6	69.4	65.7	64.0	65.2	64.9	73.8	72.8	67.8	68.4
H10-C9-N11-C16	60.3	59.6	−167.6	−167.2	−61.1	−61.3	59.4	57.4	−157.5	−154.1	−25.5	−40.1
C9-N11-C16-H17	55.5	56.4	56.1	56.8	52.4	52.5	55.5	56.3	54.7	53.3	53.5	53.7
C9-N11-C16-H18	174.3	175.0	173.7	174.4	170.8	170.9	174.2	175.0	171.8	170.2	171.6	171.9
C9-N11-C16-H19	−65.2	−64.4	−66.6	−66.0	−68.1	−68.2	−65.4	−64.6	−67.7	−69.5	−68.1	−67.7

[a] Labels refer to Figures 1 and 2.

Table 2. Relative zero-point corrected energies, dipole moments, and rotational constants of equilibrium ADMCPA conformers as computed via B3LYP/6-311++G(d,p).

Conformer Designation	ΔE (kcal/mol)	μ (Debye)	Rotational Constants (GHz)		
trans conformers					
t-A	—[a]	2.56	4.81	0.76	0.68
t-B	0.2	2.53	3.21	0.93	0.76
t-C	4.4	2.53	2.85	0.99	0.81
t-D	4.4	2.40	4.07	0.79	0.73
t-E	4.8	2.88	5.03	0.73	0.71
t-F	5.0	2.98	3.31	0.85	0.79
cis conformers					
c-A	—[b]	2.95	2.32	1.31	1.15
c-B	1.0	2.87	2.69	1.14	0.88
c-C	4.3	1.94	2.28	1.28	1.02
c-D	4.7	1.74	2.92	0.99	0.92
c-E	5.4	2.87	2.50	1.14	0.96
c-F	6.2	2.64	4.09	0.86	0.78

[a] Zero-point corrected energy is –415.401984 Hartrees.
[b] Zero-point corrected energy is –415.399113 Hartrees.

The relative energies of the lowest energy *trans*- and *cis*-ADMCPA conformers also deserve note. That is, despite *c*-A having the stabilizing amine-azide interaction found in DMAZ, it is still 1.8 kcal/mol higher in energy than the lowest energy *trans*-ADMCPA structure (where this interaction is precluded). The accuracy of the energy calculations is assumed to be from 1 to 3 kcal/mol, so the true energy ordering is uncertain. But it may be found that the two isomers yield different (overall) reaction exothermicities in an otherwise similar system.

With 19 atoms and C_s symmetry, all ADMCPA conformers have 51 normal modes. Frequency values and (integrated) infrared (IR) intensities for transitions to all modes of each conformer are provided in Tables 3 and 4. Lacking experimental mid-IR absorption spectra with which to compare, the results are considered to have limited value at this time, and so are not discussed in detail. However, they do indicate that if ADMCPA molecules are synthesized, the acquisition of mid-IR absorption spectra in the range from 400 to 900 cm^{-1} will reveal which structures are present in the sample. Simulating mid-IR absorption spectra ($I(\nu)$) by modeling vibrational band contours (due to rotational line structure) with a Lorentzian lineshape,

$$I(\nu) = \sum_j A_j \frac{\gamma/\pi}{(\nu_j - \nu)^2 + \gamma^2}, \quad (1)$$

where A_j is the integrated absorption for a transition to the j^{th} normal mode and γ (equal 10 cm^{-1}) is the lineshape width at half-maximum, Figure 4 shows that the presence of *cis*-ADMCPA will be identifiable by the presence of a feature at about 590 cm^{-1}, and that *c*-A and *c*-B will be identified/distinguished by the concomitant appearance of features near either 650 cm^{-1} or 700 cm^{-1}. The presence of a feature at 447 cm^{-1}, on the other hand, will identify the presence of *trans*-ADMCPA.

Table 3. Harmonic vibrational frequencies and integrated IR intensities for *trans*-ADMCPA conformers.

Mode	Conformer											
	t-A		*t*-B		*t*-C		*t*-D		*t*-E		*t*-F	
	ν	A	ν	A	ν	A	ν	A	ν	A	ν	A
1	33	0.0	34	0.2	35	0.0	31	0.0	33	0.1	30	0.1
2	85	0.4	89	0.5	56	0.5	56	0.5	43	0.2	49	0.3
3	136	1.1	107	0.4	103	1.3	121	0.6	124	0.3	108	0.0
4	159	0.8	192	1.2	194	0.1	154	3.1	179	0.6	209	2.3
5	225	1.2	222	1.2	227	0.9	230	1.4	234	0.7	225	0.2
6	242	0.3	243	0.0	249	0.3	245	0.8	249	0.4	252	0.3
7	278	4.7	270	1.2	266	2.4	279	0.6	268	1.5	258	1.4
8	308	1.5	328	1.0	327	5.1	327	3.1	292	3.0	323	2.9
9	389	3.6	389	10.6	391	12.8	391	8.0	379	9.8	381	11.2
10	406	4.9	401	5.6	400	1.8	400	4.1	426	1.9	424	3.6
11	447	2.1	446	1.7	459	2.1	460	1.3	464	1.8	458	1.6
12	490	0.4	492	1.9	506	5.5	508	2.2	505	5.9	504	4.3
13	554	9.1	549	8.4	544	5.8	555	8.9	556	8.4	552	7.4
14	654	14.2	645	13.5	642	20.4	645	14.3	659	15.6	639	13.9
15	774	8.5	785	6.3	762	8.2	756	14.8	740	4.9	753	10.5
16	839	1.3	829	7.1	816	6.7	832	7.9	825	15.9	818	3.1
17	929	36.4	929	25.1	863	34.5	903	15.6	901	12.9	892	35.3
18	952	9.9	934	17.4	931	3.8	932	8.4	915	6.4	918	8.4
19	969	6.5	977	9.4	961	12.1	942	5.5	966	19.4	975	10.4
20	1031	18.0	1032	15.3	1027	13.5	1024	21.8	1012	19.6	1016	16.7
21	1056	6.8	1055	9.8	1061	16.0	1059	14.5	1040	22.9	1057	22.2
22	1062	16.7	1079	11.5	1081	5.8	1070	11.1	1061	15.3	1060	9.8
23	1094	0.8	1094	10.2	1100	33.0	1087	11.9	1094	10.2	1103	5.4
24	1106	10.2	1111	2.3	1113	7.5	1111	28.6	1109	24.1	1110	23.2
25	1117	4.3	1116	4.2	1121	5.8	1114	6.8	1115	5.2	1119	10.1
26	1145	1.4	1146	2.4	1147	4.7	1147	1.3	1151	5.9	1155	12.2
27	1186	17.5	1184	16.0	1174	10.5	1175	8.8	1175	10.6	1175	9.0
28	1223	4.5	1224	5.2	1219	15.3	1219	18.7	1215	20.8	1209	7.5
29	1243	20.3	1241	20.8	1243	10.8	1243	13.8	1241	10.1	1238	10.6
30	1311	6.9	1309	8.4	1319	13.3	1314	10.4	1309	34.8	1310	28.1
31	1314	38.4	1314	12.1	1331	113.8	1325	195.5	1325	172.7	1326	129.0
32	1331	210.2	1331	164.0	1350	40.6	1347	21.1	1354	39.3	1354	51.9
33	1413	4.1	1406	28.3	1416	17.0	1420	4.0	1425	1.6	1419	13.2
34	1441	0.0	1440	0.0	1442	0.6	1442	0.7	1441	0.4	1441	0.3
35	1463	4.9	1465	6.1	1473	0.3	1472	0.8	1471	2.3	1472	2.5
36	1483	7.4	1483	7.1	1484	5.4	1484	13.6	1484	10.6	1483	21.1
37	1488	9.7	1485	21.4	1485	28.2	1486	10.4	1493	13.7	1488	19.4
38	1498	6.2	1497	9.6	1500	5.1	1500	7.1	1499	11.6	1499	8.1
39	1499	21.3	1498	20.4	1502	25.0	1502	22.6	1501	15.6	1501	15.6
40	1515	10.4	1514	10.5	1517	16.6	1518	17.3	1517	15.2	1516	14.8
41	2234	699.9	2232	626.8	2228	648.9	2229	686.9	2232	676.5	2232	645.5
42	2922	49.3	2922	43.8	2914	64.4	2911	75.0	2916	62.8	2918	63.0
43	2929	149.3	2929	145.1	2927	98.3	2931	97.8	2929	116.8	2931	120.4
44	3024	48.2	3025	51.2	3056	31.8	3056	34.1	3056	33.6	3056	32.4
45	3059	21.8	3058	22.2	3065	33.6	3065	33.8	3067	26.0	3067	25.3
46	3061	39.9	3061	38.6	3098	25.2	3098	25.0	3098	22.5	3098	22.7
47	3103	14.6	3101	21.2	3111	17.5	3109	20.0	3107	33.8	3107	31.7
48	3105	37.9	3105	31.1	3124	3.3	3122	2.9	3127	5.6	3130	5.8
49	3129	8.9	3132	8.1	3130	22.7	3128	27.2	3136	4.9	3135	4.2
50	3134	8.5	3135	8.6	3136	11.7	3134	9.2	3141	16.2	3139	19.3
51	3222	4.2	3225	3.5	3219	5.1	3218	5.6	3215	6.6	3218	5.6

Notes: ν = cm^{-1}; A = kilometers per mole.

Table 4. Harmonic vibrational frequencies and integrated IR intensities for *cis*-ADMCPA conformers.

Mode	Conformer											
	c-A		*c*-B		*c*-C		*c*-D		*c*-E		*c*-F	
	ν	*A*	ν	*A*	ν	*A*	ν	*A*	ν	*A*	ν	*A*
1	50	0.1	32	0.0	40	0.1	27	0.1	26	0.1	28	0.3
2	85	0.0	77	0.3	69	0.8	75	1.5	60	0.1	56	0.4
3	135	2.2	149	1.1	151	3.9	102	0.9	158	1.5	114	0.5
4	191	1.0	166	1.4	172	1.4	189	5.9	183	1.7	213	3.8
5	227	1.9	227	0.2	214	1.1	213	0.8	240	1.1	233	2.7
6	241	0.2	240	0.4	228	0.5	225	1.2	263	2.4	257	0.9
7	257	0.4	259	0.7	282	7.7	280	2.5	288	1.1	265	1.5
8	334	5.6	329	5.1	297	1.5	291	5.3	322	3.8	311	1.2
9	386	1.3	373	5.0	384	7.6	382	2.2	378	2.2	372	1.5
10	409	1.6	398	3.1	403	1.0	402	3.2	419	1.1	420	1.9
11	496	2.8	494	1.1	501	1.5	500	3.2	498	4.9	500	4.2
12	537	11.2	545	8.2	535	7.5	548	7.9	553	8.5	551	9.5
13	592	3.8	589	5.4	588	21.9	605	0.7	574	9.2	592	1.7
14	701	17.0	656	18.4	656	6.7	628	39.0	662	20.1	637	13.5
15	750	5.0	753	5.8	712	2.7	718	2.9	737	7.5	724	9.3
16	788	14.5	808	0.8	782	7.8	808	10.9	781	4.4	794	33.0
17	838	12.6	839	14.3	827	6.7	831	7.4	829	3.7	840	1.3
18	938	39.7	938	36.3	909	13.6	918	12.0	933	15.9	931	24.3
19	976	1.7	987	6.0	965	26.2	990	21.1	955	18.2	964	6.0
20	1042	9.1	1049	7.9	1054	2.8	1029	3.6	1038	5.1	1023	6.5
21	1056	7.1	1058	7.1	1065	12.7	1060	5.0	1062	30.7	1039	18.1
22	1066	20.5	1074	10.8	1074	4.4	1069	14.7	1073	7.4	1061	28.8
23	1096	6.5	1102	4.3	1105	19.0	1103	9.3	1092	19.2	1093	9.8
24	1117	4.0	1116	4.2	1116	3.3	1109	3.8	1115	3.3	1115	5.4
25	1130	1.0	1129	0.5	1126	7.7	1115	4.1	1119	6.1	1125	1.4
26	1137	2.5	1149	4.9	1154	1.7	1159	1.8	1147	12.8	1158	14.8
27	1186	16.1	1183	14.4	1171	8.5	1173	5.7	1174	11.1	1177	12.6
28	1201	2.1	1213	11.3	1212	8.1	1214	23.0	1214	11.7	1228	27.6
29	1242	20.9	1242	21.5	1252	19.4	1251	19.6	1237	13.6	1234	12.4
30	1314	6.1	1314	5.2	1329	33.6	1324	52.3	1316	41.0	1320	70.8
31	1361	98.4	1337	44.3	1349	31.1	1350	34.8	1327	45.1	1338	28.8
32	1389	38.8	1373	137.8	1370	108.3	1368	124.6	1366	111.3	1378	141.5
33	1397	7.0	1397	24.7	1404	13.2	1406	10.7	1418	9.2	1425	2.7
34	1441	0.5	1441	0.2	1443	0.7	1440	0.6	1442	1.2	1442	2.3
35	1467	3.5	1467	9.0	1474	2.6	1472	3.2	1474	8.5	1471	6.6
36	1482	8.4	1482	5.7	1483	10.2	1480	13.9	1485	6.9	1485	10.7
37	1485	10.2	1484	16.9	1485	18.1	1483	9.9	1489	21.5	1490	19.5
38	1497	6.1	1497	10.4	1497	8.0	1497	9.6	1500	7.0	1501	3.8
39	1500	15.8	1498	11.3	1507	3.5	1509	1.9	1507	2.6	1505	8.7
40	1514	10.2	1514	10.0	1523	17.9	1525	18.6	1518	17.1	1518	15.8
41	2239	518.1	2229	628.6	2231	636.2	2233	731.5	2233	628.4	2234	753.1
42	2922	45.2	2914	45.0	2940	65.4	2961	59.6	2920	63.6	2918	43.3
43	2929	157.9	2922	159.0	2959	74.8	2967	77.8	2928	154.6	2926	156.4
44	3008	73.3	2994	72.1	3050	36.9	3049	42.6	3058	29.0	3056	33.0
45	3061	20.6	3059	27.5	3060	37.8	3057	38.3	3068	28.5	3068	34.7
46	3064	30.8	3064	30.4	3091	24.3	3086	30.1	3099	27.4	3098	29.9
47	3105	21.8	3105	20.0	3096	16.7	3096	14.5	3105	15.5	3106	12.2
48	3113	18.1	3110	27.9	3102	22.6	3100	24.8	3121	10.8	3122	8.5
49	3123	5.8	3117	18.4	3112	29.9	3112	33.1	3128	11.1	3141	3.4
50	3183	9.2	3130	9.7	3133	14.1	3131	11.9	3148	15.2	3143	18.5
51	3210	7.8	3220	5.8	3218	5.9	3218	5.8	3217	6.9	3213	7.7

Notes: ν = cm^{-1}; *A* = kilometers per mole.

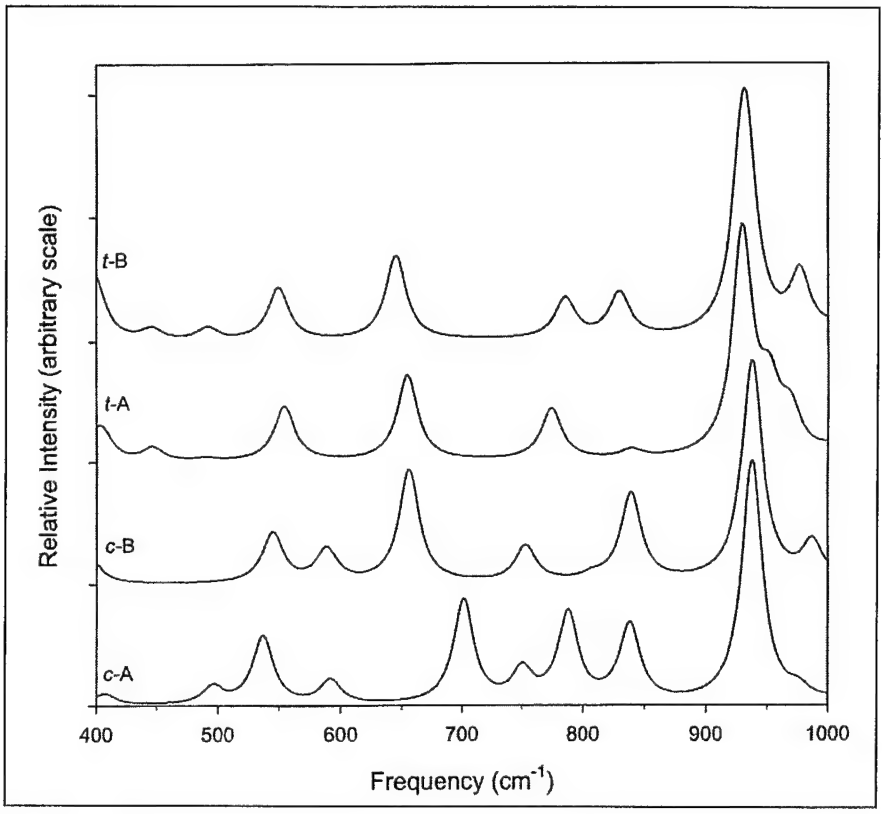

Figure 4. Simulated mid-IR absorption spectra for low energy *trans*-ADMCPA and *cis*-ADMCPA structures.

3.2 AMCBA and ACPA

The equilibrium AMCBA and ACPA structures identified through this study are shown in Figures 5 and 6, respectively. The conformers in these limited sets were obtained via geometry optimizations started with structures expected (based on the ADMCPA characterizations) to be energetically favored. Shielding configurations in *trans* isomers were also sought. Complete geometric parameters and normal mode details for the structures in these figures are provided in the Appendix. Briefly, as in DMAZ and *cis*-ADMCPA, the *cis* isomers of AMCBA and ACPA have configurations with interacting amine and azide groups that are 1.0 kcal/mol lower in energy than otherwise similar conformers. Thus, a population dominated by a shielded configuration is expected for the *cis* forms. As for *trans*-AMCBA and *trans*-ACPA, the increasing flexibility of their rings allows closer proximity of the azide and amine groups than in *trans*-ADMCPA; the N2-N(amine) distance measuring their separation decreases from 4.29 Å in *trans*-ADMCPA [*t*-B] to 3.71 Å in *trans*-AMCBA and 3.16 Å in *trans*-ACPA. The N2-N(amine) separation in *trans*-ACPA is very close to the 3.07-Å N2-N(amine) separation in the lowest energy DMAZ structure, limiting the author's interest in further characterization of this molecule.

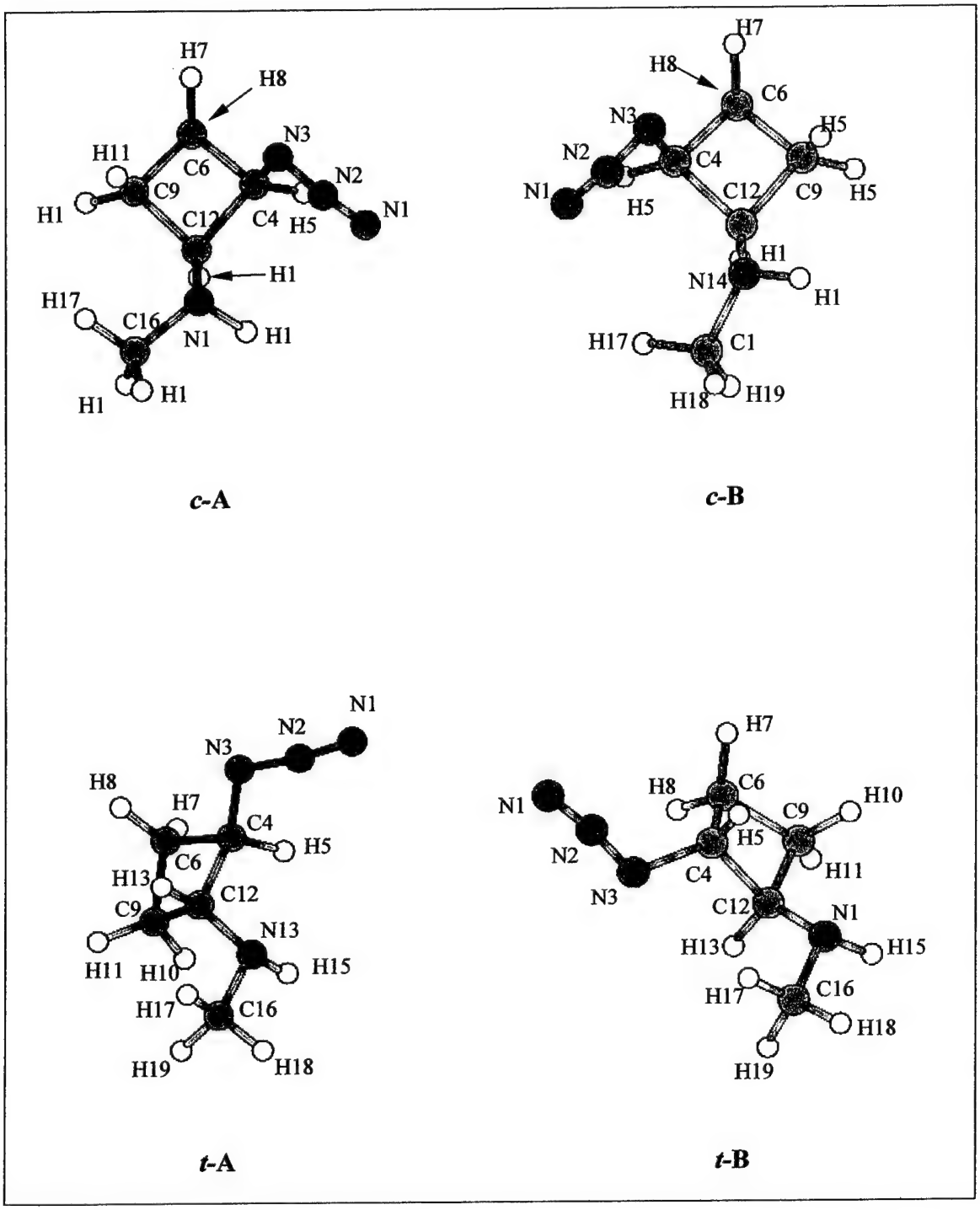

Figure 5. Equilibrium AMCBA conformers. (Arrows point to atoms hidden in the perspective shown.)

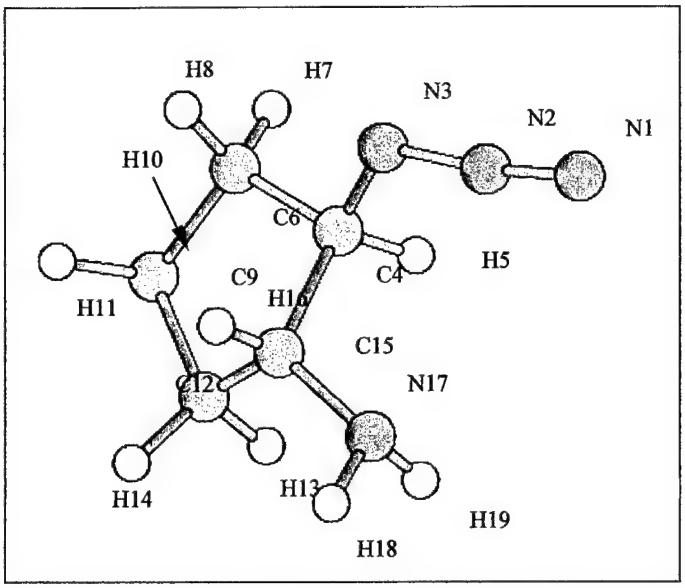

Figure 6. An equilibrium ACPA conformer. (Arrow points to atom hidden in the perspective shown.)

3.3 Gas-Phase Heats of Formation

Table 5 shows the gas-phase $\Delta H_f(298)$ estimates obtained for various alkanes, aliphatic amines, CINCH compounds, and the ADMCPA isomers based on calculated $\Delta H_r(0)$ values for isodesmic reactions. However, one of the concerns with such estimates, i.e., an inability to identify and correct systematic error [13], raises a question about their reliability and requires comment. The author attempted to address this issue by constructing isodesmic reactions in a consistent manner, i.e., forming the molecule of interest and H_2 from reactants with accepted $\Delta H_f(298)$ values. For alkanes and aliphatic amines with accepted $\Delta H_f(298)$ values, this method yields reasonably accurate, but systematically high (0–3.5 kcal/mol), estimates. This suggests that the method's values can, in fact, be rationalized and was the basis for extending the method to obtain $\Delta H_f(298)$ estimates for the azide-functionalized molecules in the table.

Another general concern in predicting $\Delta H_f(298)$ via theoretical results for isodesmic reaction schemes—namely, the necessity of good experimental heat of formation values for all (assumed) knowns—proves to be an issue for the azide-functionalized fuels and also requires comment. First, the bonds in the azido group are unique in nature—i.e., they are not reliably represented as single, double, or triple bonds, or by other "common" bonds—and thus the isodesmic schemes must include an azido compound as a reactant. Unfortunately, the only simple azide compound with a reliable heat of formation value is hydrozoic acid (HN_3). Heats of formation for methyl azide and ethyl azide would have been valuable, but published experimental values could not be found, and there are indications that values obtained with the G2 method are from 2 to 3 kcal/mol too low [15]. Thus the ability to compare values from different isodesmic schemes and identify systematic errors is limited. Based on the author's "best estimates" for the $\Delta H_f(298)$'s of methylazide and ethylazide and an experimentally obtained $\Delta H_f(298)$ for

Table 5. Gas-phase $\Delta H_f(298)$ estimates.

Compound	ZPE	H(298)-H(0)		$\Delta H_f(0)$		$\Delta H_f(298)$		Diff.	Isodesmic Reaction Scheme
	(a.u.)	JANNAF (kcal/mol)	Calc (kcal/mol)	Exp[a] (kcal/mol)	Calc (kcal/mol)	Exp[b] (kcal/mol)	Calc (kcal/mol)		
C(solid)		0.25		0.0		0.00			
H_2	-1.169506	2.02	2.07	0.0		0.00			
N_2	-109.554124	2.07	2.07	0.0		0.00			
Ammonia	-56.548462	2.40	2.40	-9.3		-10.97			
Methane	-40.489427	2.40	2.39	-16.0		-17.90			
Cyclopropane	-117.850067		2.71	17.0		12.75			
Hydrazoic acid	-164.814684		2.62	71.8		70.30			
Ethane	-79.782286		2.78	-16.3	-15.0	-20.23	-18.9	1.3	$CH_4+CH_4 \rightarrow$ Ethane$+H_2$
Butane	-158.374256		4.23	-23.0	-19.5	-30.14	-26.7	3.5	2 Ethane$\rightarrow$Butane$+H_2$
Methylamine	-95.830097		2.75	-1.8	-1.3	-5.49	-5.0	0.5	$CH_4+NH_3 \rightarrow MeNH_2+H_2$
Ethylamine	-135.129229		3.37	-5.6	-4.7	-11.00	-10.1	0.9	$CH_4+MeNH_2 \rightarrow EtNH_2+H_2$
					-5.5		-10.9	0.1	Ethane$+NH_3 \rightarrow EtNH_2+H_2$
Cyclopropylamine	-173.202101		3.39	24.1	24.6	18.42	19.0	0.5	$(CH_2)_3+NH_3 \rightarrow CpNH_2+H_2$
Dimethylamine	-135.117679		3.37	0.9	2.5	-4.50	-2.9	1.6	$CH_4+MeNH_2 \rightarrow Me_2NH+H_2$
Diethylamine	-213.715623		4.95	-8.8	-5.3	-17.30	-13.8	3.5	Ethane$+EtNH_2 \rightarrow Et_2NH+H_2$
Trimethylamine	-174.408125		4.02	1.4	3.4	-5.70	-3.7	2.0	$CH_4+Me_2NH \rightarrow Me_3N+H_2$
Methyl azide	-204.103331		3.40	75.5	75.5	(73)	72.4	(-0.6)	$CH_4+HN_3 \rightarrow MeN_3+H_2$
Ethyl azide	-243.402659		4.07	71.1	71.1	(68)	66.4	(-1.6)	Ethane$+HN_3 \rightarrow EtN_3+H_2$
1-azidobutane	-321.995173		5.28		64.0	59.9	55.9	-4.0	Butane$+HN_3 \rightarrow BuN_3+H_2$
MMAZ	-338.036614		5.56		86.5		78.8		$CH_4+EtNH_2+HN_3 \rightarrow MMAZ+2H_2$
DMAZ	-377.325354		6.33		88.0	75.6	78.8	3.2	Me_2NH+Ethane$+HN_3 \rightarrow DMAZ+2H_2$
CPAZ	-415.40821		6.53		112.6		103.4		$(CH_2)_3+EtNH_2+HN_3 \rightarrow CPAZ+2H_2$
trans-ADMCPA	-415.401984		6.66		115.7		106.7		$Me_2NH+(CH_2)_3+HN_3 \rightarrow ADMCPA+2H_2$
cis-ADMCPA	-415.399113		6.56		117.5		108.4		$Me_2NH+(CH_2)_3+HN_3 \rightarrow ADMCPA+2H_2$

[a] "Experimental" $\Delta H_f(0)$ values are the sum of experimental (exp) $\Delta H_f(298)$ values and calculated (calc) H(298)-H(0) values.
[b] Values in parentheses are estimates proposed by the author based on consideration of results published by Rogers and McCafferty [15] and Lee et al. [16].

1-azidobutane [16], the aliphatic azide *$\Delta H_f(298)$* values appear to be underpredicted. But since these underpredictions are coupled with (expected) slight overpredictions for the (isodesmic) formation of secondary and tertiary amines from primary and secondary amines, the author expects that the Table 5 *$\Delta H_f(298)$* estimates for the aliphatic amine azides from these schemes will prove to be reasonably accurate. An experimental value for DMAZ has been established [2, 3] and indicates that the theoretically based prediction is approximately 3 kcal/mol (5%) too high. However, given the lack of corroborating evidence for the experimental value, this issue is considered an open one.

4. Molecular Mechanics Methods and Results

In addition to the gas-phase properties characterized, the author was interested in estimating condensed-phase densities and heats of vaporization for each ADMCPA isomer. Coupled with the gas-phase heats of formation determined, such property predictions can be employed in

calculations to predict a fuel's performance in a propulsion system. Having been employed successfully by Bunte and Sun for predicting/estimating the density of nitrate esters [17], an approach for obtaining condensed-phase properties based on the Molecular Simulations, Inc. (MSI, now Accelrys, Inc.) suite of molecular modeling codes and its COMPASS force field [18] was desired. However, COMPASS force field parameters for azide atom types had not been developed at the time of the study, so the use of "azide analogs" in the simulation routines had to be considered. The properties of notional azide compounds are commonly predicted based on their halogen analogs, and a specific approach for predicting densities was suggested by the work of Lee et al. [16], who found that the (experimentally determined) densities of ω-azidoalkanes are nearly identical to those of their monochloride analogs. In addition, these researchers found that the heats of vaporization of ω-azidoalkanes are close to those of their monobromide analogs.

To establish that the correspondences observed by Lee et al. would be found computationally, MD simulations with the monochloride and monobromide analogs of DMAZ, CPAZ, MMAZ, and 1-azidobutane were set up and run. The simulations were performed on cubic three-dimensional periodic cells containing 1080–1100 atoms (56–72 molecules) constructed by the Amorphous Cell module of Insight II. (Amorphous Cell builds cells according to a modified Markov process, incorporating rotational isomeric state probabilities modified to account for nonlocal [long-range] interactions [19, 20].) Eight different cells with an initial target density of 0.9 g/cm^3 were built for each compound, the length of cube edges being ~25 Å for monochloride compounds and ~23 Å for monobromide compounds. A group-based cut-off method with tail correction was employed to evaluate nonbond interactions. The cut-off method assumes that the radial distribution functions converge to unity beyond the cut-off distance. The cut-off distance was specified to be 10 Å for all compounds except the CPAZ analogs, where a 10.5-Å cutoff was employed.

The simulations consisted of three stages, the dynamics in all cases being modeled with Verlet velocity integration [21] and Andersen temperature control [22]. Berendsen pressure control [23] was employed for constant pressure simulations. The first stage was a 30,000-step, 1-fs/step, constant volume and temperature (NVT) "pre-equilibration" simulation run to relieve large stresses (inadvertently) introduced by the cell packing procedure. The second stage of the procedure was a 30,000-step, 1-fs/step constant pressure and temperature (NPT) simulation that allowed the cell to equilibrate. The final stage was a 50,000-step, 1-fs/step NPT simulation during which data was recorded.

Table 6 compares the densities of the monochloride analogs of DMAZ, CPAZ, MMAZ, and 1-azidobutane vs. experimentally determined values for the corresponding azides. The computationally determined density for 1-chlorobutane is observed to be nearly identical to its experimentally determined value and that of 1-azidobutane. (Given that the COMPASS force field parameters for the atom types relevant to 1-chlorobutane were probably developed with a

Table 6. Condensed-phase property estimates.

Compound	Density		$\Delta H_v(298)$		$\Delta H_f(298)$			
	MD (g/cm^3)	Exp (g/cm^3)	MD (kcal/mol)	Exp (kcal/mol)	Calc (kcal/mol)	Exp (kcal/mol)	Calc (cal/g)	Exp (cal/g)
1-azidobutane[a]		0.883		9.17	46.5	50.7	470	510
1-chlorobutane[a]	0.882 ± 0.003	0.886	7.8	8.01				
1-bromobutane[a]			7.5	8.79				
2-azido-N-methylethanamine (MMAZ)[b]		0.970			69		690	
2-chloro-N-methylethanamine	0.980 ± 0.003		9.6					
2-bromo-N-methylethanamine			9.2					
2-azido-N,N dimethylethanamine (DMAZ)[b]		0.933		9.4	69	66	610	580
2-chloro-N,N dimethylethanamine	0.955 ± 0.004		9.5					
2-bromo-N,N dimethylethanamine			8.8					
2-azido-N-cyclopropylethanamine (CPAZ)[b]		0.993			94		750	
2-chloro-N-cyclopropylethanamine	0.981 ± 0.006		9.1					
2-bromo-N-cyclopropylethanamine			9.7					
trans-2-chloro-N,N-dimethylcyclopropanamine (*trans*-ADMCPA analog)								
1 enantiomer only	0.946 ± 0.006							
Racemic mixture	0.953 ± 0.005		9.5		97		770	
cis-2-azido-N,N-dimethylcyclopropanamine (*cis*-ADMCPA analog)								
1 enantiomer only	0.992 ± 0.006							
Racemic mixture	1.000 ± 0.005		10.6		98		790	
Monomethylhydrazine (MMH)[c]		0.883		9.6		13.1		284

[a] Experimental data are from Lee et al. [16].
[b] Experimental data are from Thompson et al. [2, 3].
[c] Experimental data are as reported in the Schmidt [1] compendium.

training set consisting of ω-alkylchlorides, the good agreement was expected.) The computationally determined densities for the monochloride analogs of MMAZ, DMAZ, and CPAZ are also observed to be in reasonable agreement with experimentally determined values for the corresponding azide. The approach predicts that the density of *trans*-ADMCPA will be 0.945 g/cm^3, a value that is slightly lower than that predicted for DMAZ (0.955 g/cm^3). The density of *cis*-ADMCPA is predicted to be 1.00 g/cm^3, a value that is even higher than that predicted for CPAZ (0.98 g/cm^3).

Table 6 also presents estimates for the heats of vaporization of the monochloride and monobromide analogs of DMAZ, CPAZ, MMAZ, and 1-azidobutane. It is observed that the values for the monochloro and monobromo analogs of DMAZ and 1-azidobutane are similar to, but lower than, the values observed experimentally for the corresponding azides. Since the heats of vaporization determined for the monochloride and monobromide analogs are similar, the effort needed to perform a separate set of simulations with bromide analogs will not be undertaken in the future. Being a byproduct of simulations necessary to predict densities, the heats of vaporization derived from monochloride analogs are "free," and thus provide an easily obtained reference point. In the present case, however, it is observed that most of the values in the table cluster near DMAZ's experimentally determined value of 9.4 kcal/mol, and this value

was employed by the author in calculating all of the condensed-phase heats of formation given in Table 6. The potential error associated with this approach is expected to be less than ±2 kcal/mol.

5. Ballistic Properties

With estimates for condensed-phase heats of formation and densities, it is possible to calculate and compare the specific impulses (I_{SP}) and density impulses (D^*I_{SP}) that MMAZ, DMAZ, CPAZ, and the ADMCPA isomers will produce when combined with an oxidizer. Table 7 compares optimized I_{SP} values from NASA-Lewis rocket calculations [24] for a system in which the oxidizer is an IRFNA "mixture." (The oxidizer mixture is one employed by AMCOM for such comparisons.) It is observed that the optimized I_{SP} values for the aliphatic amine azides are nearly identical to each other and less than 1% lower than the value obtained for MMH. Moreover, with higher densities than MMH, their D^*I_{SP}'s are predicted to be higher.

6. Synthesis Possibilities

The author has no (relevant) experience in the art of synthetic organic chemistry, but wanted to at least attempt to address the possibility of synthesizing ADMCPA. A literature search of synthesis routes for aliphatic amine azides revealed a large number of possibilities, with a relatively recent review of the preparation of azide compounds written by Schriven and Turnball being particularly instructive [25]. Of the approaches identified via this survey, the most intriguing to the author was suggested by the work of Benalil et al. [26]. Based on synthesizing desired 1,2 aminoazides by treating "appropriate" 1,2 aminoalcohols with triphenylphosphorous (PPh_3), diethyl azodicarboxylate (DEAD), and HN_3—i.e., the (modified) Mitsunobu reaction [27]—this approach should be readily testable because an appropriate 1,2 aminoalcohol for ADMCPA, namely *trans*-2-hydroxy-N,N-dimethylcyclopropanamine, has already been synthesized by Armstrong and Cannon [28]. Since the modified Mitsunobu reaction converts alcohols to azides through inversion of configuration, successful conversion of *trans*-2-hydroxy-N,N-dimethylcyclopropanamine via this approach will probably produce *cis*-ADMCPA.

7. Discussion

The superior performance of hydrazine and its methylated derivatives compared to other hypergols can generally be attributed to three characteristics: short ignition delays, high

Table 7. NASA-Lewis thermochemical code I_{SP} and D^*I_{SP} predictions for various fuels.[a]

Compound	O/F	I_{SP}			%Δ
		Throat (s)	Exit (s)	D^*I_{SP}[b] ($lb_f \cdot s/in^3$)	
MMAZ	2.0	112.9	284.8		
	2.2	111.4	285.4		
	2.4	109.9	284.4	10.1	+10
	2.6	108.5	281.0		
	2.8	107.1	276.7		
	3.0	105.7	272.0		
DMAZ	2.0	113.7	281.1		
	2.2	112.9	283.3		
	2.4	111.7	284.4	9.8	+7
	2.6	110.4	284.4		
	2.8	109.1	282.8		
	3.0	107.8	279.5		
CPAZ	2.0	113.9	281.3		
	2.2	113.2	283.6		
	2.4	112.0	284.8		
	2.6	110.8	284.9	10.1	+10
	2.8	109.5	283.9		
	3.0	108.2	281.1		
cis-ADMCPA	2.0	114.3	282.5		
	2.2	113.4	284.6		
	2.4	112.3	285.6		
	2.6	111.0	285.7	10.3	+12
	2.8	109.7	284.5		
	3.0	108.5	281.7		
trans-ADMCPA	2.0	114.2	282.1		
	2.2	113.3	284.2		
	2.4	112.2	285.3		
	2.6	110.9	285.4	9.8	+7
	2.8	109.6	284.3		
	3.0	108.4	281.5		
MMH	2.0	115.6	284.7		
	2.2	115.0	286.8		
	2.4	113.9	288.0		
	2.6	112.4	288.1	9.2	—
	2.8	110.9	285.7		
	3.0	109.5	280.8		

[a] Results for "infinite-area" combustor problem with 2000-psia chamber pressure and equilibrium chemistry. The subsonic area ratio is 15.0, and the supersonic area ratio is 14.175.

[b] For consistency, in all cases (except MMH), the density predictions obtained via the molecular modeling computations are employed to calculate D^*I_{SP}.

densities, and high specific impulses, the shortcoming of most alternatives being long ignition delays. Given that aliphatic azides are not hypergolic and that the ignition delays of aliphatic amines are much longer than those of hydrazine and its derivatives, the short ignition delays produced by (the aliphatic amine azide) DMAZ are surprising, and identifying the mechanisms that underlie this phenomenon could be useful in designing fuels with even shorter ignition delays.

Since aliphatic azides are not hypergolic, but do undergo (explosive) exothermic unimolecular decomposition if raised to a sufficiently high temperature, and aliphatic amines are hypergolic but "slow," in the absence of detailed knowledge about DMAZ's molecular structure, a "working hypothesis" was suggested. That hypothesis was that exothermic proton transfer from nitric acid to the amine, which is more nucleophilic than the azide, was jump-starting the azide decomposition, and the azide decomposition was accelerating the otherwise slow secondary reactions involved in pure amine oxidation. This hypothesis was consistent with the observation of ammonium nitrate salts in combustion residue [3], and observed differences in the performance 2-azidoethanamines with different amine substituents, shorter ignition delays found for fuels whose amines would be expected to be stronger bases. Not surprisingly, this hypothesis led AMCOM to focus on synthesizing fuels with more a more nucleophilic amine.

The genesis of this study was the finding that in DMAZ's lowest energy configuration, the azide group sterically shields the lone pair electrons associated with the amine nitrogen [4]. Given the experimentally indicated importance of proton transfer to this site, the author initially assumed that shielding would reduce a compound's reactivity and therefore contribute to increasing ignition delays. Thus, his interest was in identifying compounds that would prevent shielding. Through the course of this study, however, several observations led the author to consider the possibility that the amine-azide interaction in the shielding configuration is actually the enabling mechanism. First, given the fact that close to 50% of DMAZ's amine sites will be shielded from proton attack at room temperature and that DMAZ is competitive with Aerozine 50, it would be imprudent to ignore this possibility. Second, though (aliphatic) azides are not known as hypergols, the azide group has two lone pair sites and nitric acid hydrogen bonds (exothermically) to these sites in the gas phase. Calculations for an as yet incomplete study to characterize DMAZ-nitric acid complexes indicate that hydrogen-bonding to azide sites is only slightly less than the exothermic than the hydrogen-bonding at amine sites. In addition, though enhancing the amine's basicity would almost certainly reduce ignition delays, there is the potential that any increase in amine basicity will be offset by an enhancement of the amine-azide interaction and an increase in shielding. (Such an effect is suggested by preliminary results from ongoing theoretical characterizations of CPAZ and MMAZ.) If enhancement of the azide group's basicity through the azide-amine interaction is the enabling mechanism, then *cis*-ADMCPA could yield very short ignition delays. The author hopes that the promise of the ADMCPA isomers that is indicated in the computational characterizations presented is sufficient

to pursue their synthesis, as experimental testing with them should clarify the influence of the azide-amine interaction and the azide's basicity on the ignition process.

As a final note, the possibility of using a CH_2 group to bridge the ethyl group carbons of DMAZ was investigated because of the obvious similarities between the 2-azidocycloalkanamines and DMAZ and CPAZ, but the bridge can presumably be made with groups other than CH_2, NH and O being two possibilities. A stable structure based on the former—an aziridine—is shown in Figure 7. However, the author does not have enough knowledge of small heterocyclic organic compounds to even guess as to whether their properties will be similar to DMAZ or CPAZ, so he made no attempt to further characterize such alternatives. Certainly, property estimates for such alternatives could be calculated if considered warranted.

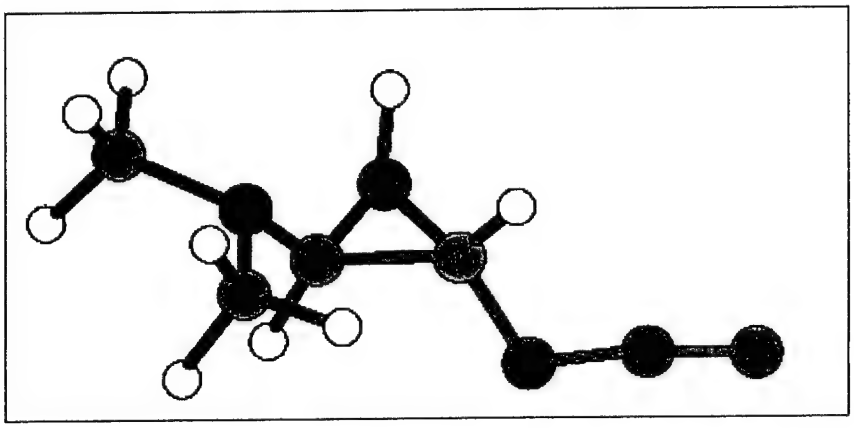

Figure 7. An equilibrium 3-azido-2-dimethylaminoaziridine conformer.

8. Summary

Fuels based on 2-azidocycloalkanamines are proposed as means of obtaining hydrazine-alternative hypergols with ignition delays shorter than those observed for DMAZ. The geometric parameters and normal modes for a number of 2-azidocycloalkanamines with $C_5H_{10}N_4$ stoichiometry were characterized through the use of DFT, and MD simulations performed with the halogen analogs of ADMCPA, DMAZ, CPAZ, and MMAZ were employed to predict liquid densities and heats of vaporization. I_{SP} and D^*I_{SP} values predicted based on the DFT and MD results, coupled with the possibility of shorter ignition delays, suggest that the ADMCPA isomers merit further consideration as alternatives to DMAZ or MMH in hypergolic propulsion system applications.

9. References

1. Schmidt, E. W. *Hydrazine and Its Derivatives: Preparation, Properties, and Applications.* New York: John Wiley & Sons, Inc., 2001.

2. Thompson, D. M., B. F. Wilson, and W. Stephenson. "Hypergolic Azide Liquid Fuels." JANNAF 28th Propellant Development and Characterization Subcommittee Meeting, 1999.

3. Thompson, D. M. Personal communications. U.S. Army Aviation and Missile Command, Redstone Arsenal, AL, 1999.

4. McQuaid, M. J., K. L. McNesby, B. M. Rice, and C. F. Chabalowski. "Density Functional Theory Characterization of the Structure and Gas-Phase, Mid-Infrared Absorption Spectrum of 2-azido–N,N-dimethylethanamine (DMAZ)." *Journal of Molecular Structure: THEOCHEM*, vol. 587, pp. 199–218, 2002.

5. Frisch, M. J., G. W. Trucks, H. B. Schlegel, G. E. Scuseria, M. A. Robb, J. R. Cheeseman, V. G. Zakrzewski, J. A. Montgomery, R. E. Stratmann, J. C. Burant, S. Dapprich, J. M. Millam, A. D. Daniels, K. N. Kudin, M. C. Strain, O. Farkas, J. Tomasi, V. Barone, M. Cossi, R. Cammi, B. Mennucci, C. Pomelli, C. Adamo, S. Clifford, J. Ochterski, G. A. Petersson, P. Y. Ayala, Q. Cui, K. Morokuma, D. K. Malick, A. D. Rabuck, K. Raghavachari, J. B. Foresman, J. Cioslowski, J. V. Ortiz, B. B. Stefanov, G. Liu, A. Liashenko, P. Piskorz, I. Komaromi, R. Gomperts, R. L. Martin, D. J. Fox, T. Keith, M. A. Al-Laham, C. Y. Peng, A. Nanayakkara, C. Gonzalez, M. Challacombe, P. M. W. Gill, B. G. Johnson, W. Chen, M. W. Wong, J. L. Andres, M. Head-Gordon, E. S. Replogle, and J. A. Pople. Gaussian 98. Revision A.4, Gaussian, Inc., Pittsburgh PA, 1998.

6. Becke, A. D. "Density-Functional Thermochemistry 3: The Role of Exact Exchange." *Journal of Chemical Physics*, vol. 98, pp. 5648–5652, 1993.

7. Lee, C., W. Yang, and R. G. Parr. "Development of the Colle-Salvetti Correlation-Energy Formula Into a Functional of the Electron-Density." *Physical Review B*, vol. 37, pp. 785–789, 1988.

8. Miehlich, B., A. Savin, H. Stoll, and H. Preuss. "Results Obtained With the Correlation-Energy Density Functionals of Becke and Lee, Yang and Parr." *Chemical Physics Letters*, vol. 157, pp. 200–206, 1989.

9. Clark, T., J. Chandrashakar, G. W. Spitznagel, and P. V. R. Schleyer. "Efficient Diffuse Function-Augmented Basis-Sets for Anion Calculations 3, the 3-21+G Basis Set for 1st-Row Elements, Li-F." *Journal of Computational Chemistry*, vol. 4, pp. 294–301, 1983.

10. McLean, A. D., and G. S. Chandler. "Contracted Gaussian-Basis Sets for Molecular Calculations. 1. 2nd Row Atoms, Z=11-18." *Journal of Chemical Physics*, vol. 72, pp. 5639–5648, 1980.

11. Krishnan, R., J. S. Binkley, R. Seeger, and J. A. Pople. "Self-Consistent Molecular-Orbital Methods. 20. Basis Set for Correlated Wave-Functions." *Journal of Chemical Physics*, vol. 72, pp. 650–654, 1980.

12. Curtiss, L. A., K. Raghavachari, G. W. Trucks, and J. A. Pople. "Gaussian-2 Theory for Molecular-Energies of 1st-Row and 2nd-Row Compounds." *Journal of Chemical Physics*, vol. 94, pp. 7221–7230, 1991.

13. Foresman, J. B., and A. Frisch. *Exploring Chemistry With Electronic Structure Methods*. Pittsburgh, PA: Gaussian, Inc., 1996.

14. Chase, M. W. *NIST-JANNAF Thermochemical Tables*. 4th Edition, Gaithersburg, MD: American Chemical Society and American Institute of Physics for the National Institute of Standards and Technology, 1998.

15. Rogers, D. W., and F. J. McLafferty. "G2 Ab Initio Calculations of the Enthalpy of Formation of Hydrazoic Acid, Methyl Azide, Ethyl Azide, Methyl Amine, and Ethyl Amine." *Journal of Chemical Physics*, vol. 103, pp. 8302–8303, 1995.

16. Lee, A., C. K. Law, and A. Makino. "Aerothermochemical Studies of Energetic Liquid Materials. 3. Approximate Determination of Some Thermophysical and Chemical Properties of Organic Azides." *Combustion and Flame*, vol. 78, pp. 263–274, 1989.

17. Bunte, S., and H. Sun. "The Molecular Modeling of Energetic Materials: Parameterization and Validation of Nitrate Esters in the COMPASS Force Field." *Journal of Physical Chemistry B*, vol. 104, pp. 2477–2489, 2000.

18. Sun, H. "COMPASS: An Ab Initio Force-Field for Condensed Phase Applications: Overview With Details on Alkane and Benzene Compounds." *Journal of Physical Chemistry B*, vol. 102, pp. 7338–7364, 1998.

19. Theodorou, D. N., and U. W. Suter. "Atomistic Modeling of Mechanical Properties of Polymeric Glasses." *Macromolecules*, vol. 18, p.139, 1986.

20. Meirovitch, H. "Computer-Simulation of Self-Avoiding Walks—Testing the Scanning Method." *Journal of Chemical Physics*, vol. 79, pp. 502–508, 1983.

21. Swope, W. C., H. C. Andersen, P. H. Berens, and K. R. Wilson. "A Computer-Simulation Method for the Calculation of Equilibrium-Constants for the Formation of Physical Clusters of Molecules—Application to Small Water Clusters." *Journal of Chemical Physics*, vol. 76, pp. 637–649, 1982.

22. Andersen, H. C. "Molecular Dynamics Simulations at Constant Pressure and/or Temperature." *Journal of Chemical Physics*, vol. 72, pp. 2384–2393, 1980.

23. Berendsen, H. J. C., J. P. M. Postma, W. F. van Gunsteren, A. DiNola, and J. R. Haak. "Molecular-Dynamics With Coupling to an External Bath." *Journal of Chemical Physics*, vol. 81, pp. 3684–3690, 1984.

24. McBride, B. J., and S. Gordon. "Computer Program for Calculation of Complex Chemical Equilibrium Compositions and Applications. II. Users Manual and Program Description." NASA Reference Publication 1311, NASA Lewis Research Center, Cleveland, OH, 1996.

25. Schriven, E. F., and K. Turnball. "Azides: Their Preparation and Synthetic Uses." *Chemical Reviews*, vol. 88, pp. 297–368, 1988.

26. Benalil, A., B. Carboni, and M. Vaultier. "Synthesis of 1,2-Aminoazides. Conversion to Unsymmetrical Vicinal Diamines by Catalytic Hydrogenation or Reductive Alkylation With Dichloroboranes." *Tetrahedron*, vol. 47, pp. 8177–8194, 1991.

27. Loibner, H., and E. Zbiral. "Reactions With Organophosphorous Compounds. 41. New Preparative Methods Using Triphenylphosphine-Diethyl Azodicarboxylate-Hydroxy-Compound." *Helvetica Chimica Acta*, vol. 59, pp. 2100-2113, 1976.

28. Armstrong, P. D., and B. C. Cannon. "Small Ring Analogs of Acetylcholine: Synthesis and Configurations of Cyclopropane Derivatives." *Journal of Medicinal Chemistry*, vol. 13, pp. 1037–1039, 1970.

INTENTIONALLY LEFT BLANK.

Appendix. Details From 2-Azido-N-methylcyclobutanamine (AMCBA) and 2-Azidocyclopentanamine (ACPA) Theoretical Characterizations

This Appendix provides tables summarizing the theoretical characterizations of *cis* and *trans* forms of 2-azido-N-methyl-cyclobutanamine (AMCBA) and a *trans* isomer of 2-azido-cyclopentanamine (ACPA). Table A-1 presents the geometric parameters for the AMCBA conformers shown in Figure 5, and Table A-2 presents their relative zero-point corrected energies, dipole moments, and rotational constants. Table A-3 presents the normal mode frequencies and integrated infrared (IR) intensities for transitions to these modes for the AMCBA structures. Table A-4 presents the geometric parameters for the ACPA conformer shown in Figure 6, and Table A-5 presents its normal mode frequencies and the integrated IR intensities for transitions to these modes. The dipole moment for the ACPA conformer is 3.94 Debye, and its rotational constants are 3.07, 1.15, and 0.88 GHz. Its zero-point corrected energy is –415.448209 Hartrees.

Table A-1. Geometric parameters for equilibrium AMCBA conformers as computed via B3LYP/6-311++G(d,p).

	Conformers[a]			
Parameter	***c*-A**	***c*-B**	***t*-A**	***t*-D**
Bond Length (in Angstroms)				
N1-N2	1.136	1.135	1.135	1.136
N2-N3	1.228	1.230	1.230	1.229
N3-C4	1.475	1.471	1.469	1.474
C4-C6	1.546	1.546	1.542	1.553
H5-C4	1.095	1.095	1.097	1.095
C6-C9	1.553	1.553	1.553	1.553
H7-C6	1.089	1.089	1.090	1.090
H8-C6	1.091	1.091	1.092	1.092
C9-C12	1.550	1.546	1.570	1.549
H10-C9	1.092	1.092	1.094	1.092
H11-C9	1.091	1.091	1.090	1.090
C12-C4	1.567	1.577	1.549	1.546
H13-C12	1.105	1.103	1.094	1.103
N14-C12	1.447	1.441	1.442	1.449
H15-C14	1.016	1.012	1.015	1.015
C16-C14	1.464	1.459	1.462	1.463
H17-C16	1.093	1.094	1.094	1.092
H18-C16	1.092	1.092	1.092	1.092
H19-C16	1.103	1.103	1.102	1.102
Simple Angles (in Degrees)				
N3-N2-N1	173.0	172.4	173.1	173.7
C4-N3-N2	116.8	116.8	116.8	116.5
H5-C4-N3	109.9	110.2	110.4	110.7
C6-C4-N3	108.8	108.9	115.7	118.8
H7-C6-C4	115.3	115.5	117.3	117.3
H8-C6-C4	111.5	111.6	110.3	110.9
C9-C6-C4	89.1	89.1	88.5	87.7
H10-C9-C6	111.3	111.0	112.0	111.9
H11-C9-C6	117.9	118.3	117.6	117.6
C12-C9-C6	88.1	88.6	87.8	88.6
H13-C12-C9	108.7	109.6	109.3	110.1
N14-C12-C9	118.4	118.9	117.2	117.5
H15-N14-C12	110.0	110.9	110.4	109.4
C16-N14-C12	113.6	115.8	115.0	114.2
H17-C16-N14	109.6	109.9	109.2	109.6
H18-C16-N14	109.3	109.5	109.4	109.4
H19-C16-N14	113.9	113.7	114.2	113.7
Dihedral Angles (in Degrees)				
C4-N3-N2-N1	168.9	-166.3	174.4	-179.3
H5-C4-N3-N2	-56.1	58.5	-36.8	42.4
C6-C4-N3-N2	173.7	-171.1	164.2	-88.7
H7-C6-C4-N3	24.2	-24.7	96.5	101.5
H8-C6-C4-N3	149.7	-150.4	-29.2	-25.0
C9-C6-C4-N3	-96.1	95.7	-142.0	-137.8
H10-C9-C6-C4	92.1	-92.5	-92.1	-92.5
H11-C9-C6-C4	-139.9	139.7	140.6	139.6
C12-C9-C6-C4	-19.4	19.2	20.0	19.4
H13-C12-C9-C6	-88.5	88.7	89.0	89.2
N14-C12-C9-C6	140.9	-141.1	-141.5	-139.6
H15-N14-C12-C9	-172.5	-30.2	49.2	-50.9
C16-N14-C12-C9	64.5	-158.7	76.4	175.0
H17-C16-N14-C12	-64.7	-65.2	-62.7	-64.4
H18-C16-N14-C12	177.6	177.4	179.7	177.6
H19-C16-N14-C12	56.2	55.8	58.2	56.0

[a] Labels refer to Figure 5.

Table A-2. Relative zero-point corrected energies, dipole moments, and rotational constants for equilibrium AMCBA conformers as computed via B3LYP/6-311++G(d,p).

Conformer Designation[a]	**ΔE (kcal/mol)**	**μ (Debye)**	**Rotational Constants (GHz)**		
trans conformers					
t-A	—[b]	3.54	2.24	1.15	0.80
t-B	0.2	2.90	2.41	1.10	0.80
cis conformers					
c-A	1.2	3.25	2.10	1.43	0.92
c-B	—[c]	3.38	2.03	1.57	0.99

[a] See Figure 5.
[b] Zero-point corrected energy is –415.414753 Hartrees.
[c] Zero-point corrected energy is –415.410703 Hartrees.

Table A-3. Harmonic vibrational frequencies and integrated IR intensities for equilibrium AMCBA conformers.

Mode	Conformer[a]							
	c-A		*c*-B		*t*-A		*t*-B	
	ν	*A*	ν	*A*	ν	*A*	ν	*A*
1	58	0.2	64	0.1	35	0.2	27	0.0
2	97	1.3	79	1.0	84	0.2	77	1.9
3	105	0.5	104	1.0	106	0.7	116	1.7
4	173	1.3	175	0.9	172	0.8	147	0.9
5	192	0.4	183	0.6	197	0.4	190	0.1
6	225	0.3	251	1.4	236	1.0	235	0.4
7	298	1.7	273	2.9	278	4.2	332	1.9
8	367	6.3	373	3.2	368	8.0	355	8.5
9	439	5.7	417	4.0	449	3.1	419	5.5
10	519	4.6	530	13.8	491	3.2	474	2.7
11	559	12.0	559	16.0	548	5.1	547	8.8
12	647	24.3	633	48.0	552	4.8	578	17.6
13	699	2.0	667	21.1	680	39.8	672	7.9
14	751	8.3	695	10.5	735	44.0	738	84.3
15	777	59.0	755	1.0	818	19.5	811	3.0
16	840	4.3	837	7.9	822	3.3	820	4.9
17	905	5.7	903	3.1	909	5.5	924	3.1
18	937	1.3	933	1.8	933	1.3	927	1.3
19	950	8.4	962	2.8	991	12.0	997	38.2
20	1004	6.4	996	4.3	1007	14.5	1007	0.1
21	1041	18.1	1045	9.6	1050	16.3	1049	2.9
22	1076	9.4	1078	8.6	1066	7.5	1078	11.9
23	1116	5.6	1114	1.4	1102	12.4	1107	1.2
24	1138	1.9	1143	4.0	1149	2.0	1146	2.0
25	1173	13.3	1169	24.6	1162	38.2	1170	38.0
26	1201	22.5	1187	11.4	1199	19.1	1207	1.8
27	1212	1.1	1235	3.5	1211	2.9	1212	2.6
28	1246	0.8	1248	0.7	1236	0.6	1242	0.2
29	1266	1.1	1262	2.2	1252	0.3	1255	1.8
30	1268	5.1	1272	9.8	1265	0.7	1263	2.0
31	1294	6.4	1286	9.5	1280	15.3	1284	2.0
32	1335	138.4	1332	123.6	1329	114.4	1329	135.3
33	1344	65.9	1342	58.1	1356	64.1	1353	77.0
34	1379	34.4	1383	22.3	1394	65.7	1402	55.0
35	1459	2.0	1463	0.1	1458	1.9	1460	3.0
36	1475	7.3	1472	4.3	1483	3.8	1474	3.1
37	1480	2.6	1476	8.3	1491	14.6	1482	4.3
38	1493	8.8	1493	8.4	1496	6.3	1493	5.1
39	1496	6.4	1495	6.5	1506	9.1	1502	10.1
40	1518	11.2	1517	12.7	1522	27.1	1518	13.4
41	2231	609.7	2232	583.4	2233	684.5	2230	740.2
42	2907	71.8	2935	36.2	2953	90.8	2937	41.4
43	2938	114.2	2944	129.0	3009	19.0	2947	103.0
44	3025	47.7	3026	45.3	3040	18.2	3041	14.6
45	3059	7.7	3052	25.2	3050	23.3	3056	34.8
46	3062	50.9	3053	34.4	3054	40.5	3062	35.5
47	3068	31.2	3067	32.2	3065	25.3	3062	18.2
48	3102	23.1	3100	24.7	3097	25.6	3102	29.7
49	3111	16.3	3103	24.8	3102	26.2	3105	13.5
50	3127	27.0	3126	24.7	3120	34.7	3120	34.3
51	3506	0.2	3556	3.3	3516	0.4	3521	0.7

[a] See Figure 5.

Notes: ν = cm^{-1}; *A* = kilometers per mole.

Table A-4. Geometric parameters for an equilibrium ACPA conformer as computed via B3LYP/6-311++G(d,p).

Parameter[a]	
Bond Length (in Angstroms)	
N1-N2	1.134
N2-N3	1.230
N3-C4	1.475
H5-C4	1.010
C6-C4	1.534
H7-C6	1.091
H8-C6	1.093
C9-C6	1.557
H10-C9	1.092
H11-C9	1.092
C12-C9	1.549
H13-C12	1.097
H14-C12	1.093
C15-C12	1.543
C15-C4	1.542
H16-C15	1.096
N17-C15	1.458
H18-N17	1.013
H19-N17	1.016
Simple Angles (in Degrees)	
N3-N2-N1	172.2
C4-N3-N2	117.0
H5-C4-N3	109.4
C6-C4-N3	110.4
H7-C6-C4	111.9
H8-C6-C4	108.2
C9-C6-C4	105.6
H10-C9-C6	111.8
H11-C9-C6	110.3
C12-C9-C6	105.9
H13-C12-C9	110.5
H14-C12-C9	113.2
C15-C12-C9	105.1
H16-C15-C4	112.0
N17-C15-C4	111.9
H18-N17-C15	111.6
H19-N17-C15	112.8
Dihedral Angles (in Degrees)	
C4-N3-N2-N1	168.3
H5-C4-N3-N2	-38.2
C6-C4-N3-N2	-160.0
H7-C6-C4-N3	84.4
H8-C6-C4-N3	-33.3
C9-C6-C4-N3	-152.2
H10-C9-C6-C4	-114.7
H11-C9-C6-C4	126.9
C12-C9-C6-C4	6.7
H13-C12-C9-C6	-98.4
H14-C12-C9-C6	141.7
C15-C12-C9-C6	18.7
H16-C15-C4-N3	46.4
N17-C15-C4-N3	-70.7
H18-N17-C15-C4	163.3
H19-N17-C15-C4	-76.0

[a] See Figure 6.

Table A-5. Harmonic vibrational frequencies and integrated IR intensities for an ACPA conformer as computed via B3LYP/6-311++G(d,p).[a]

Mode	ν	A
1	40	0.2
2	61	0.5
3	114	0.3
4	180	1.6
5	231	29.0
6	274	1.1
7	354	7.4
8	387	11.4
9	469	4.0
10	533	3.5
11	556	9.3
12	603	1.5
13	691	11.8
14	769	11.5
15	796	75.4
16	815	43.1
17	910	4.4
18	936	16.7
19	956	3.6
20	988	7.0
21	1028	6.5
22	1072	9.5
23	1092	0.5
24	1120	6.4
25	1136	10.6
26	1195	1.4
27	1244	1.9
28	1265	0.5
29	1283	2.0
30	1317	0.5
31	1319	0.6
32	1328	2.9
33	1335	124.9
34	1344	2.5
35	1376	65.3
36	1428	12.0
37	1490	0.8
38	1497	5.2
39	1519	7.1
40	1660	34.4
41	2236	655.3
42	2980	20.6
43	3012	19.5
44	3034	31.1
45	3048	26.7
46	3058	35.5
47	3070	24.6
48	3083	17.3
49	3102	51.0
50	3499	0.5
51	3586	3.2

[a] See Figure 6.

Notes: ν = cu^{-1}; A = kilometers per mole.

REPORT DOCUMENTATION PAGE

Form Approved
OMB No. 0704-0188

1. AGENCY USE ONLY *(Leave blank)*	2. REPORT DATE	3. REPORT TYPE AND DATES COVERED
	September 2002	Final, May 2001–May 2002

4. TITLE AND SUBTITLE
Computational Characterization of 2-Azidocycloalkanamines: Notional Variations on the Hypergol 2-Azido-N,N-Dimethylethanamine (DMAZ)

5. FUNDING NUMBERS
611102.H43

6. AUTHOR(S)
Michael J. McQuaid

7. PERFORMING ORGANIZATION NAME(S) AND ADDRESS(ES)
U.S. Army Research Laboratory
ATTN: AMSRL-WM-BD
Aberdeen Proving Ground, MD 21005-5066

8. PERFORMING ORGANIZATION REPORT NUMBER
ARL-TR-2806

9. SPONSORING/MONITORING AGENCY NAMES(S) AND ADDRESS(ES)

10.SPONSORING/MONITORING AGENCY REPORT NUMBER

11. SUPPLEMENTARY NOTES

12a. DISTRIBUTION/AVAILABILITY STATEMENT
Approved for public release; distribution is unlimited.

12b. DISTRIBUTION CODE

13. ABSTRACT*(Maximum 200 words)*

The fuel 2-azido-N,N-dimethylethanamine (DMAZ) has shown considerable promise as a replacement for hydrazine-based fuels in hypergolic propulsion systems, but the ignition delays observed for DMAZ-inhibited red fuming nitric acid (IRFNA) systems are longer than those for monomethylhydrazine-IRFNA systems. This report considers the potential of 2-azidodocycloalkanamine-based fuels for addressing this issue. Such molecules have two stereochemically distinct isomers, one of which prevents the azide group from "shielding" the amine lone pair electrons from proton attack. The other promotes such shielding. Since shielding likely influences the manner in which nitric acid reacts with amine-azide fuels, the ignition delays for the isomers may be different, and it is possible that one of the isomers will yield shorter ignition delays than DMAZ. To support consideration of the synthesis and development of 2-azido-N,N-dimethylcyclopropanamine (ADMCPA) equilibrium structures are identified and their gas-phase heats of formations estimated via density functional theory-based calculations. In addition, ADMCPA isomer condensed-phase densities and heats of vaporization are estimated via molecular dynamics simulations performed with halogen analogs. Combined and employed to predict ballistic properties, the computational results indicate that the ADMCPA isomers merit further investigation as hypergols. A suggestion for synthesizing cis?ADMCPA is also proffered.

14. SUBJECT TERMS
hypergolic fuels, DMAZ, density functional theory, molecular dynamics, 2-azidocycloalkanamines

15. NUMBER OF PAGES
36

16. PRICE CODE

17. SECURITY CLASSIFICATION OF REPORT	18. SECURITY CLASSIFICATION OF THIS PAGE	19. SECURITY CLASSIFICATION OF ABSTRACT	20. LIMITATION OF ABSTRACT
UNCLASSIFIED	UNCLASSIFIED	UNCLASSIFIED	UL

INTENTIONALLY LEFT BLANK.